CHAPTER 11

Predict the critical load of rectangular concrete-filled steel tube columns with ultra high strength concrete with software ANSYS

Phan Van-Phuc, Pham Ngoc-Minh, Nguyen Thi Dieu-Thuy and Cao Thi-Hao
Department of Civil Engineering, Vinh University, Vinh, Nghe An, Vietnam

1. Introduction

Ultra high performance concrete (UHPC) is a more advanced development of traditional fiber reinforced concrete (FRP). Unlike glass fiber concrete (GFRC) which is concerned with bending strength to manufacture decorative products, UHPC is concerned with the compressive performance of the material. In the early 1970s experts predicted that the practical limit of ready-mix concrete would certainly not exceed the load capacity of 11,000 psi. However, up to now, there have been many projects using concrete with compressive strength up to 20,000 psi.

Concrete-filled steel tubular (CFST) structure has numerous structural benefits and has been widely used in civil engineering structures. Overall, CFST columns exploit various advantages of steel and concrete materials by combining them together (Choi & Xiao, 2010). Therefore, CFST columns offer some inherent good properties, such as high load-carrying capacity, high seismic resistance, aesthetic appearance, reduced cross-section, high resistance under fire and explosion, and work faster (Chen et al., 2010; Morino & Tsuda, 2003). Furthermore, core concrete slows down local warping of steel pipes thus eliminates the need for concrete cast reinforcement thus resulting in rapid construction (Hu et al., 2011).

CFST columns have many different types of cross-sections, such as circles, squares and rectangles, ellipses, and polygons. Particularly for the circular section CFST column, much research has been done on its

Multi-Hazard Vulnerability and Resilience Building
ISBN 978-0-323-95682-6
https://doi.org/10.1016/B978-0-323-95682-6.00005-X

structure and method of determining its behavior as in the studies of Schneider (Schneider, 1998), Shams et al. (Shams & Saadeghvaziri, 1997), De Nardin và El Debs (Hassanein et al., 2018), và Viet-Linh Tran et al. (Tran et al., 2020). CFST column is widely used because it can achieve more load carrying capacity and provides higher yield rear axle ductility due to significant restraining effect. Round section CFST columns have been adopted by design standards such as AS/NZS 5100.6 (Hicks et al., 2017), Eurocode 4 (Johnson, 2012), ANSI (Committee, 2010), GB 50956 (GB50936-2014, 2014). Besides, CFST columns with square and rectangular cross-sections have not been studied much. With the current development of science and technology, the method of structural simulation by finite element-based software is quite popular and highly effective. One of them is ANSYS (finite element software). Many studies are showing that ANSYS is used to study construction structures. ANSYS is used to consider the performance of reinforced concrete beams (Santhakumar et al., 2007), of high-strength reinforced concrete columns (Kottb et al., 2015), of long columns with stainless steel (Al Akawai et al., 2018). When using the simulation method for structural cases with uncompressed 3-axis concrete, it is necessary to use different criteria from the working of normal concrete such as Cam-Clay, Drucker-Prager, Mohr-Coulomb, Menetrey-Willam, …. in which the Druker-Prager criterion has been used a lot and with a quite high accuracy (Kartal et al., 2012; Oztekin et al., 2016; Yu et al., 2010). However, building an accurate Drucker-Prager model needs to depend on many factors and is quite complicated (Alejano & Bobet, 2012).

To solve the above-mentioned difficult problems, this paper presents how to determine the critical load of the CFST column with square cross-section by ANSYS finite element software. This method saves the cost of the experiment as well as details the effects of specific parameters in the Drucker-Prager model in the CFST column.

2. Method

Initially, the method was conducted based on previous research results on the parameters of super high strength steel and concrete materials. Then consider the effect of the parameters on the simulation method by finite element software ANSYS WORKBENCH and select the appropriate stress-strain relationship for the analytical model. The selected texture for analysis is the experimental sample S1 in the experimental study of Ming-Xiang Xiong (Xiong et al., 2017).

2.1 Stress-strain relationship for steel materials

The stress–strain relationship of steel is shown in Fig. 11.1 (Hassanein et al., 2018) where: ε_y is the plastic deformation of the steel corresponding to the stress f_y, ε_t is the maximum strain in the yielding phase (taken as 0.005). ε_t và fu are the relative strain and maximum stress, respectively. The stress–strain relationship of steel is established by Multilinear Isotropic Hardening. Poisson's coefficient is taken as 0.3, yield strength is taken as 90% of its value.

2.2 Drucker-Prager model specifications for UHPC

In the case of concrete packed into a steel box, it is quite affected by the triaxial compressive properties, so the Drucker–Prager (DP) model for concrete is suitable according to previous studies (Fam & Rizkalla, 2001; Hu et al., 2003; Liang, 2009; Tran et al., 2020). To use the DP model, it is necessary to define many parameters (Alejano & Bobet, 2012). For this study, the simulation method also uses the Drucker–Prager model for UHPC but considers the influence of the parameters differently from previous studies (Fig. 11.2). The poisson coefficient of UHPC material is taken as 0.25 (Liew & Xiong, 2012; Tran et al., 2020). The initial elastic modulus was obtained according to the data from the experiment (Xiong et al., 2017). For cases where the elastic modulus is not available, the following formulas can be obtained:

In this study, the main values for using the DP model are the strength of uniaxial, biaxial compressive material, the strength of uniaxial tensile materials, the yield phase, the softening phase of the material (Oystein Grostad, 2018). uniaxial tensile strength is taken as: $f_t = 0.65 \cdot \sqrt{f'_c}$. Biaxial

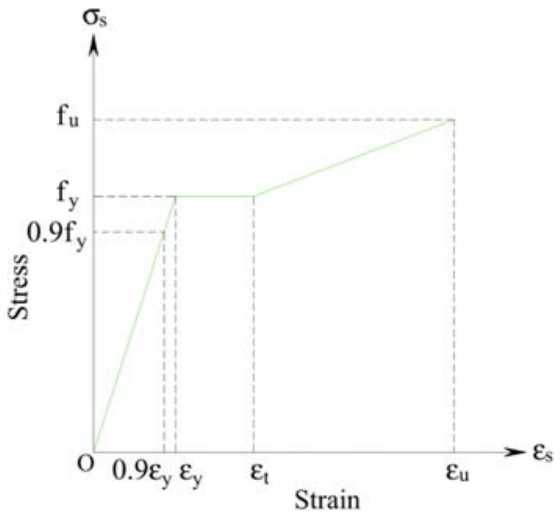

Figure 11.1 Stress-strain relationship of steel shell.

Properties of Outline Row 4: Concrete NL

	A	B	C	D	E
1	Property	Value	Unit		
2	Material Field Variables	Table			
3	Density	2300	kg m^-3		
4	Isotropic Elasticity				
5	Derive from	Young's Mo...			
6	Young's Modulus	6.2E+10	Pa		☑
7	Poisson's Ratio	0.25			
8	Bulk Modulus	4.1333E+10	Pa		
9	Shear Modulus	2.48E+10	Pa		
10	Drucker-Prager				
11	Drucker-Prager Base				
12	Uniaxial Compressive Strength	152.2	MPa		
13	Uniaxial Tensile Strength	8E+06	Pa		☑
14	Biaxial Compressive Strength	1.9E+08	Pa		☑
15	Dilatancy				
16	Tensile and Tension-Compression Dilatancy	0.25			
17	Compression Dilatancy	1			
18	Softening				
19	Active Table	Linear			
20	Plastic Strain at Uniaxial Compressive Strength	0.003			
21	Ultimate Effective Plastic Strain in Compression	0.09			☑
22	Relative Stress at Start of Nonlinear Hardening	0.4			☑
23	Residual Compressive Relative Stress	0.6			☑
24	Plastic Strain Limit in Tension	1E-05			
25	Residual Tensile Relative Stress	0.2			☑
26	Damage Evolution Law				
27	Active Table	Material Pro...			
28	Tensile Fiber Stiffness Reduction	1			
29	Compressive Fiber Stiffness Reduction	1			
30	Tensile Matrix Stiffness Reduction	1			
31	Compressive Matrix Stiffness Reduction	1			

Figure 11.2 Drucker-Prager model parameters for UHPC.

compressive strength is taken as: $f_c'' = (1.1 \div 1.45) \cdot f_c'$ (Lee et al., 2017). Dilatancy coefficients are taken from 0 to 1, the coefficients of the softening and damage phase have been proposed with certain ranges of values Fig. 11.3.

2.2.1 Effect of tensile strength

The value of tensile strength is taken around the value $0.65 \cdot \sqrt{f_c'}$ to consider its influence on the ultimate load when simulating with the DP model. The relationship between the tensile strength and the ultimate load is shown in Fig. 11.4. From the results, it can be seen that the tensile strength does not have much influence on the ultimate load. The maximum change critical load value is 0.00045%.

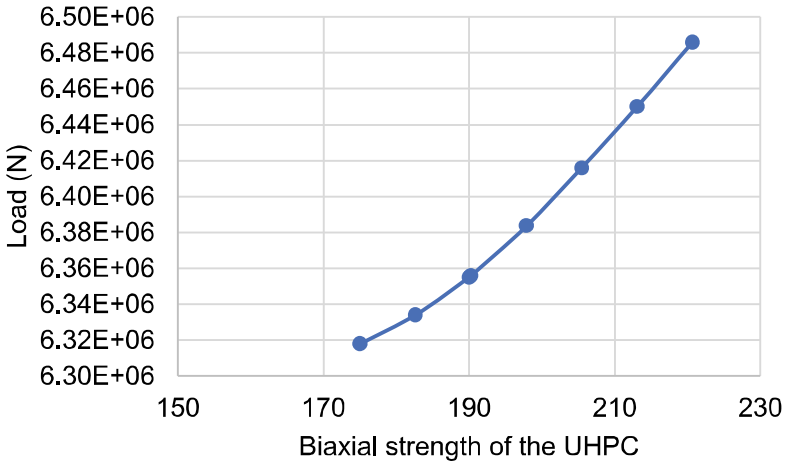

Figure 11.3 Relationship of critical load and biaxial compressive strength.

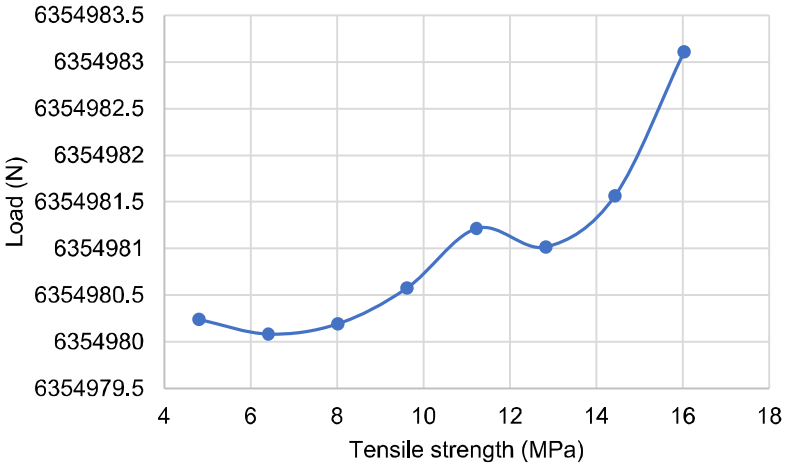

Figure 11.4 The relationship of load with tensile strength.

2.2.2 Effect of elastic modulus

Elastic modulus is considered with values in Table 11.1, the relationship of critical load and elastic modulus is shown in Fig. 11.5. The value of the critical load changes without any rule, but the change of the ultimate load when the elastic modulus changes is not significant, 0.08% maximum.

2.2.3 Effect of coefficient of friction

The values of the coefficient of friction between the UHPC core and the steel shell are considered with 0.1, 0.15, 0.2, and 0.25, respectively. The value 0.3 and the obtained results are shown in Fig. 11.6. When the coefficient of friction between UHPC and the steel plate changes, the critical load does not affect much, the largest difference is 0.083%.

Table 11.1 Elastic modulus cases.

The formula for determining the elastic modulus	According to the document
$E_c = 5700 \cdot \sqrt{f'_c}$	Mander et al. (1988)
$E_c = 4700 \cdot \sqrt{f'_c}$	ACI 318-11 (2011)
$E_c = 4730 \cdot \sqrt{f'_c}$	Popovics (1973)
$E_c = 5573 \cdot \sqrt{f'_c}$	Wu & Wang (2009)
$E_c = 3320 \cdot \sqrt{f'_c} + 6900$ (Mpa)	Liang (2009)

Where E_c, f_c are the elastic modulus, uniaxial compressive strength of UHPC, respectively.

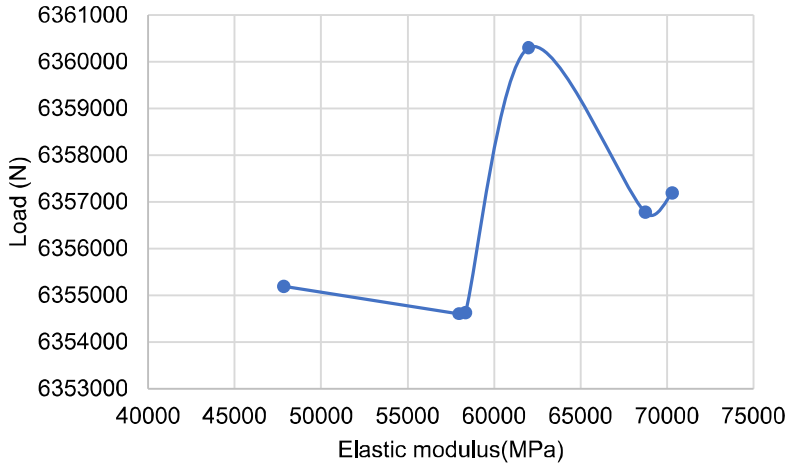

Figure 11.5 The relationship of critical load with elastic modulus.

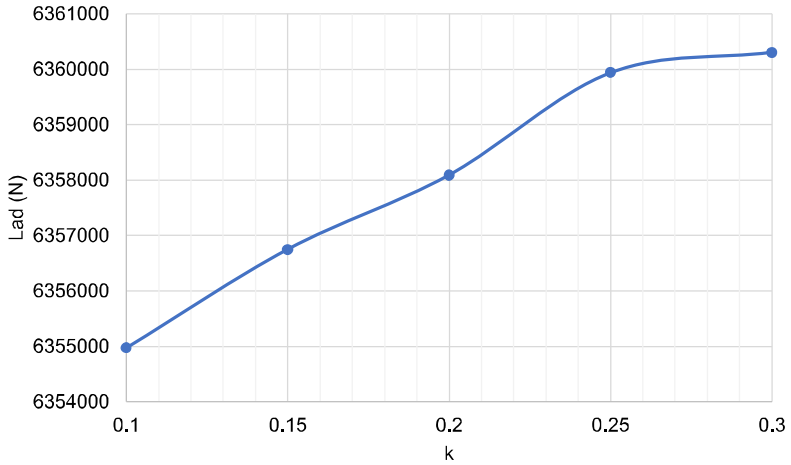

Figure 11.6 Relationship of critical load with the coefficient of friction.

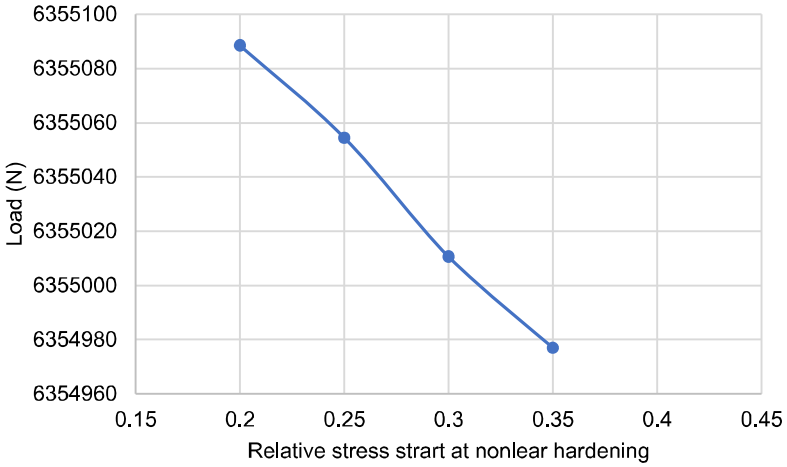

Figure 11.7 The relationship of critical load with relative stress starts at nonlinear hardening.

2.2.4 Effect of stress value at the starting position of hardening

When the value of stress at the starting position hardening occurs with values equal to 20%, 25%, 30%, 35% of the 1-axis compressive strength of UHPC, we have the result of the relationship between the critical load with the starting stress of hardening on Fig. 11.7. The resulting critical load is not affected much for this case, the maximum difference is 0.00176%. Proceeding similarly with the remaining parameters, the study obtained the results that the critical loads are almost unchanged when they change.

3. Result of critical load of CFST column with a square cross-section

From the above results, to determine the critical load of a rectangular steel column filled with high-strength concrete with ANSYS WORKBENCH, it is necessary to pay attention to the value of 2-axis compressive strength, and other values may be chosen at random in its condition to determine the critical load.

Fig. 11.8 shows that the deformation shape of the CFST column is quite similar between the simulation method by ANSYS and the experimental results (Xiong et al., 2017). The load-displacement relationship of the CFST column is shown in Fig. 11.9. Compared with the experimental results of Xiong (Xiong et al., 2017), the results of the load-displacement relationship are quite similar.

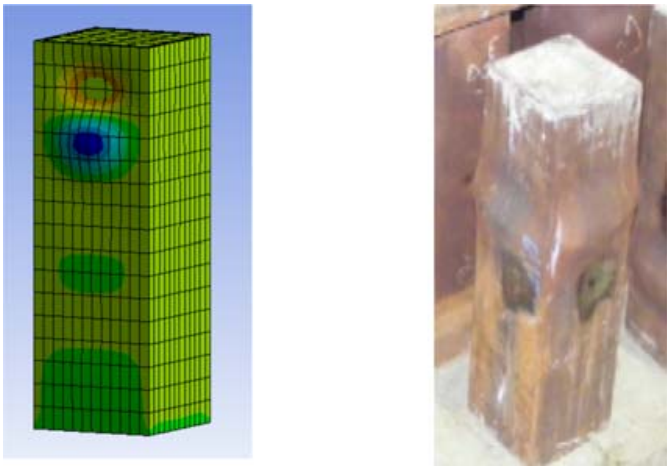

Figure 11.8 Deformation of simulation and experimental methods.

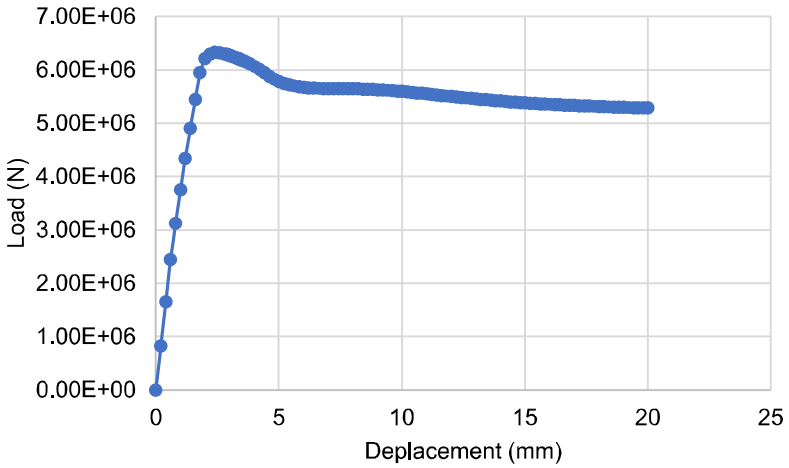

Figure 11.9 The load-displacement relationship of the CFST column.

4. Compare results

Table 11.2 shows the results of the CFST column simulation method using ANSYS Workbench, the experimental results, as well as the results from the calculation method from the current standards. Table 11.3 shows the error of CFST column critical load with other methods.

Table 11.2 CFST column critical load value of rectangular cross-section.

N_{ANSYS} (KN)	N_{TEST} (KN	N_{EC4} (KN)	N_{AISC} (KN)	$N_{ACI/AS}$ (KN)	N_{AIJ} (KN)	N_{CISC} (KN)
6334.1	6536	6428	6441	6441	6831	6435

Table 11.3 Compare the results of the simulation method with other methods.

N_{ANSYS}/N_{TEST}	N_{ANSYS}/N_{EC4}	N_{ANSYS}/N_{AISC}	$N_{ANSYS}/N_{ACI/AS}$	N_{ANSYS}/N_{AIJ}	N_{ANSYS}/N_{CISC}
0.969,109,547	0.985,392,035	0.98,340,319	0.983,403,198	0.92,725,808	0.98,432,014

5. Conclusions

The method of determining the CFST column critical load by ANSYS WORKBENCH with the Drucker–Prager model gives quite accurate results and is easy to use. Among the parameters of the Drucker–Prager model, the durability parameter of ultra high performance concrete materials under biaxial compression greatly affects the results of the analysis, while other parameters have little influence on the critical load value.

Thus, the CFST column structure, when simulated by ANSYS WORKBENCH, only needs to pay attention to the value of biaxial compressive strength and the Drucker–Prager model is enough to analyze and find the critical load of the structure.

References

GB50936-2014, (2014), "Technical code for concrete filled steel tubular structures", China Architecture & Building Press Beijing.

c ACI 318-11. (2011). *Building code requirements for structural concrete (ACI318-11).* American Concrete Institute.

AL Akawai, H. J., Aweed, K. M., & Jaber, S. A. (2018). Finite element method analysis of normal and corrosion buckling with ANSYS17 program for stainless steel 304 alloy. *International Journal of Engineering and Technology(UAE),* 7(4.7 Special Issue 7), 245—249.

Alejano, L. R., & Bobet, A. (2012). Drucker-prager criterion. *Rock Mechanics and Rock Engineering*. https://doi.org/10.1007/s00603-012-0278-2

Chen, Z., Liu, F., Zheng, H., & Xue, J. (2010). Research on the bearing capacity of recycled aggregate concrete-filled circle steel tube column under axial compression loading. In *2010 international conference on mechanic automation and control engineering* (pp. 1198—1201). IEEE.

Choi, K.-K., & Xiao, Y. (2010). Analytical model of circular CFRP confined concrete-filled steel tubular columns under axial compression. *Journal of Composites for Construction, American Society of Civil Engineers, 14*(1), 125—133.

Committee, A. (2010). *Specification for structural steel buildings (ANSI/AISC 360-10).* Chicago-Illinois: American Institute of Steel Construction.

Fam, A. Z., & Rizkalla, S. H. (2001). Confinement model for axially loaded concrete confined by circular fiber-reinforced polymer tubes. *ACI Structural Journal*. https://doi.org/10.14359/10288

Hassanein, M. F., Patel, V. I., Elchalakani, M., & Thai, H. T. (2018). Finite element analysis of large diameter high strength octagonal CFST short columns. *Thin-Walled Structures, 123*, 467—482.

Hicks, S., Uy, B., & Kang, W. H. (2017). AS/NZS 5100.6, Design of steel and composite bridges. In *Proceedings of the Austroads bridge conference, Melbourne, Australia* (pp. 3—6).

Hu, H.-T., Huang, C.-S., Wu, M.-H., & Wu, Y.-M. (2003). Nonlinear analysis of axially loaded concrete-filled tube columns with confinement effect. *Journal of Structural Engineering*. https://doi.org/10.1061/(asce)0733-9445(2003)129:10(1322)

Hu, Y. M., Yu, T., & Teng, J. G. (2011). FRP-confined circular concrete-filled thin steel tubes under axial compression. *Journal of Composites for Construction, American Society of Civil Engineers, 15*(5), 850—860.

Johnson, R. P. (2012). *Designers' guide to Eurocode 4: Design of composite steel and concrete structures: EN 1994-1-1, Thomas Telford Limited*.

Kartal, M. E., Bayraktar, A., & Basağa, H. B. (2012). Nonlinear finite element reliability analysis of Concrete-Faced Rockfill (CFR) dams under static effects. *Applied Mathematical Modelling, 36*(11), 5229–5248.

Kottb, H. A., El-Shafey, N. F., & Torkey, A. A. (2015). Behavior of high strength concrete columns under eccentric loads. *HBRC Journal, Housing and Building National Research Center, 11*(1), 22–34.

Lee, J. H., Hong, S. G., Joh, C., Kwahk, I., & Lee, J. W. (2017). Biaxial tension–compression strength behaviour of UHPFRC in-plane elements. *Materials and Structures/Materiaux et Constructions*. https://doi.org/10.1617/s11527-016-0918-1

Liang, Q. Q. (2009). Performance-based analysis of concrete-filled steel tubular beam-columns, Part I: Theory and algorithms. *Journal of Constructional Steel Research*. https://doi.org/10.1016/j.jcsr.2008.03.007

Liew, J. Y., & Xiong, D. X. (2012). Ultra-high strength concrete filled composite columns for multi-storey building construction. *Advances in Structural Engineering, 15*, 1487–1503.

Mander, J. B., Priestley, M. J. N., & Park, R. (1988). Theoretical stress-strain model for confined concrete. *Journal of Structural Engineering*. https://doi.org/10.1061/(asce)0733-9445(1988)114:8(1804)

Morino, S., & Tsuda, K. (2003). Design and construction of concrete-filled steel tube column system in Japan. *Earthquake Engineering and Engineering Seismology, 4*(1), 51–73.

Oystein Grostad, E. S. (2018). *Analysing UHPFRC beams with the help of ANSYS*.

Oztekin, E., Pul, S., & Husem, M. (2016). Experimental determination of Drucker-Prager yield criterion parameters for normal and high strength concretes under triaxial compression. *Construction and Building Materials, 112*, 725–732.

Popovics, S. (1973). A numerical approach to the complete stress-strain curve of concrete. *Cement and Concrete Research*. https://doi.org/10.1016/0008-8846(73)90096-3

Santhakumar, R., Dhanaraj, R., & Chandrasekaran, E. (2007). Behaviour of retrofitted reinforced concrete beams under combined bending and torsion: A numerical study. *Electronic Journal of Structural Engineering, 7*, 1–7.

Schneider, S. P. (1998). Axially loaded concrete-filled steel tubes. *Journal of Structural Engineering, American Society of Civil Engineers, 124*(10), 1125–1138.

Shams, M., & Saadeghvaziri, M. A. (1997). State of the art of concrete-filled steel tubular columns. *Structural Journal, 94*(5), 558–571.

Tran, V. L., Thai, D. K., & Nguyen, D. D. (2020). Practical artificial neural network tool for predicting the axial compression capacity of circular concrete-filled steel tube columns with ultra-high-strength concrete. *Thin-Walled Structures*. https://doi.org/10.1016/j.tws.2020.106720

Wu, Y.-F., & Wang, L.-M. (2009). Unified strength model for square and circular concrete columns confined by external jacket. *Journal of Structural Engineering*. https://doi.org/10.1061/(asce)0733-9445(2009)135:3(253)

Xiong, M. X., Xiong, D. X., & Liew, J. Y. R. (2017). Axial performance of short concrete filled steel tubes with high- and ultra-high- strength materials. *Engineering Structures, 136*, 494–510.

Yu, T., Teng, J. G., Wong, Y. L., & Dong, S. L. (2010). Finite element modeling of confined concrete-I: Drucker–Prager type plasticity model. *Engineering Structures, 32*(3), 665–679.